Lasers in Manufacturing Conference 2025

Micro-polishing of 4H-SiC surfaces using femtosecond laser vector beams and wobble-based scanning

Chung-Wei Cheng[a], Che Tseng[a], Jia-Fan Kuo[a]

[a] *Department of Mechanical Engineering, National Yang Ming Chiao Tung University, No. 1001, Ta Hsueh Road, Hsinchu 300, Taiwan*

Abstract

The production of 4H-SiC wafers typically involves laser slicing followed by multiple polishing steps to achieve the desired surface flatness. This study investigates the feasibility of micro-polishing 4H-SiC surfaces using femtosecond laser vector beams. In the first stage, high-fluence processing at 1.39 J/cm² was performed using femtosecond laser vector beams combined with wobble scanning to simulate the rough surface morphology produced by laser slicing, resulting in a surface roughness (Sz) of 32.3 µm. In the subsequent stage, a lower fluence of 1.25 J/cm² was employed along with a defocused beam (Z = -50 µm) for micro-polishing, which reduced the surface roughness to 9.0 µm. These results demonstrate the potential of femtosecond laser vector beams for precision micro-ablation and polishing of 4H-SiC surfaces.

Keywords: femtosecond laser; vector beam; 4H-SiC; micro-polishing

1. Introduction

Silicon carbide (SiC) has attracted significant attention due to its excellent high-temperature stability, superior thermal conductivity, and promising semiconductor properties (Casady and Johnson 1996; Mehregany et al. 1998). The fabrication of SiC wafers typically involves slicing from ingots, followed by grinding, polishing, and chemical mechanical polishing to achieve the required surface quality. Traditional polishing techniques often generate high friction and thermal energy, which may lead to localized heating and potential material damage. In contrast, femtosecond lasers with their ultrashort pulse durations and high peak power intensities enable precise micro-polishing while minimizing subsurface damage (Kažukauskas et al. 2024).

Previous studies have examined various aspects of femtosecond laser processing of SiC. Zhang et al. (2018) demonstrated that reducing the energy density of a femtosecond laser Gaussian beam to the ablation threshold can efficiently polish grooves on 4H-SiC and effectively reduce surface roughness. Zheng, Huang, and Xu (2020) compared Gaussian and vector beams and found that the concentrated energy of Gaussian beams results in a recessed central region, whereas the annular energy distribution of vector beams produces a central protrusion accompanied by an annular depression at the periphery. Li et al. (2024) further investigated SiC processing using low-energy vector beams, focusing on the formation of fine structures and the resulting surface morphology. Although recent work by Aldeiturriaga et al. (2023) on titanium and stainless steel indicated that both annular and radial polarizations can significantly lower surface roughness compared to linear polarization, the application of femtosecond laser vector beams for SiC surface polishing has not been explored.

In this study, 4H-SiC polishing experiments were conducted using femtosecond laser vector beams. The first stage simulates the rough morphology of laser-sliced 4H-SiC, and the second stage employs micro-polishing to refine the surface.

* Corresponding author. Tel.: +886-3-5712121#55126; fax:+886-3-5720634.
E-mail address: weicheng@nycu.edu.tw

2. Experimental details

2.1. Experiment setup

A polished 4H-SiC sample (UCT4SICDDP010, Atecom, Inc.) with a thickness of 350 µm and an initial roughness (Ra ≤ 0.5 nm) was used. The sample was irradiated in air using a femtosecond fiber laser (Spirit HE 1040-30-SHG) with the following specifications: wavelength 515 nm, pulse duration 323 fs, repetition rate 1 MHz, beam diameter 2.5 mm (at $1/e^2$), and maximum power 13 W. The linearly polarized beam was directed via mirrors through a segmented waveplate (SWP-532, Photonic Lattice) to convert it into an azimuthal vector beam. This beam was then scanned by a galvanometer scanner and focused onto the sample using an ƒ-theta lens. The laser was focused onto an XYZ motion platform for surface processing, achieving a focal spot diameter of 21.7 µm. Fig. 1(a) schematically shows the experimental setup, and Fig. 1(b) illustrates the conversion of a Gaussian beam into an annular beam with zero intensity at its center. Fig. 1(c) presents a photograph of the processed area.

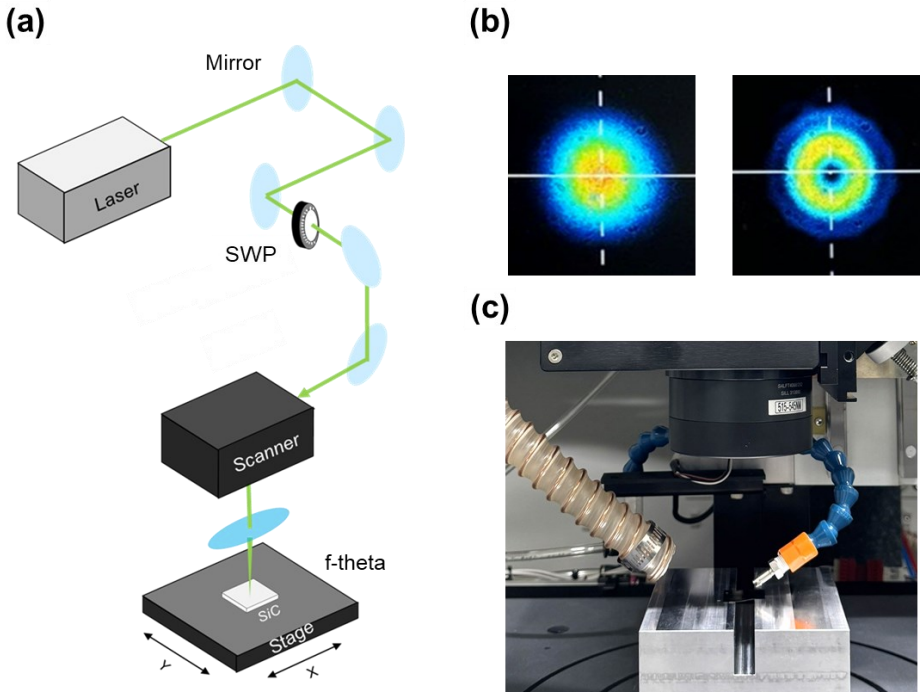

Fig. 1. (a) schematic of the experiment setup; (b) conversion of a Gaussian beam into an annular beam with zero intensity at its center; (c) photograph of the processed area

The SWP-532 consists of 12 half-wave plates arranged with continuously rotating fast-axis angles, which enables the transformation of linearly polarized light into either radial or azimuthal vector beams as illustrated in Fig. 2(a). This configuration also redistributes the Gaussian beam into an annular profile. To verify the polarization distribution, a polarizing beam splitter (PBS) was temporarily installed to separate vertical and horizontal components. By rotating the SWP, either radial or azimuthal polarization was obtained; for azimuthal polarization, two laser spots (one above and one below) were observed, while radial polarization produced spots to the left and right. Fig. 2(b) shows a fixed point processing image confirming that the beam profile at the focal spot is annular with zero intensity at its center.

The femtosecond laser was irradiated on the Si face of the material. The 4H-SiC sample was cleaned in an ultrasonic bath, first with acetone for ten minutes and then with deionization water for another ten minutes before and after the experiment. Surface morphology was characterized using a scanning electron microscope (SEM, SU-8010, Hitachi Inc.), and surface roughness was measured with a laser scanning confocal microscope (VK-X3000, Keyence Inc.). A square groove of approximately 1.2 × 1.2 mm^2 was processed, and roughness measurements were consistently taken from a central area of 0.5 × 0.5 mm^2 corresponding to the constant scanning speed region. Each parameter set was measured three times to calculate the average and standard deviation.

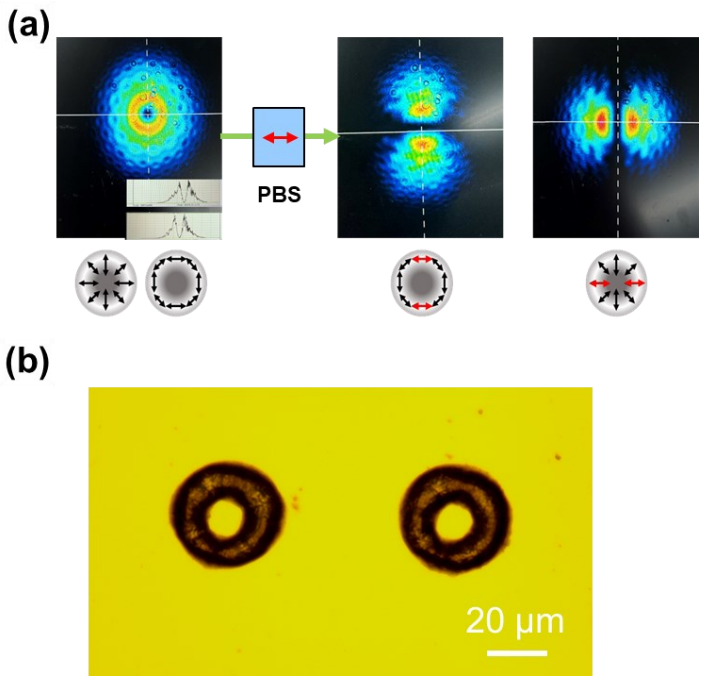

Fig. 2. (a) vector beam after polarization separation with PBS; (b) fixed-point processing image

2.2. Research method

A two-stage processing strategy was adopted (see Fig. 3). In the first stage, high-energy femtosecond laser vector beam processing combined with wobble (oscillatory) scanning was used to simulate the surface morphology of laser-sliced 4H-SiC. In the second stage, micro-polishing was performed using a low-energy femtosecond laser vector beam (azimuthal polarization) in a reciprocating scanning mode to reduce the roughness generated in the first stage. The influence of various laser parameters on the final surface roughness was systematically investigated.

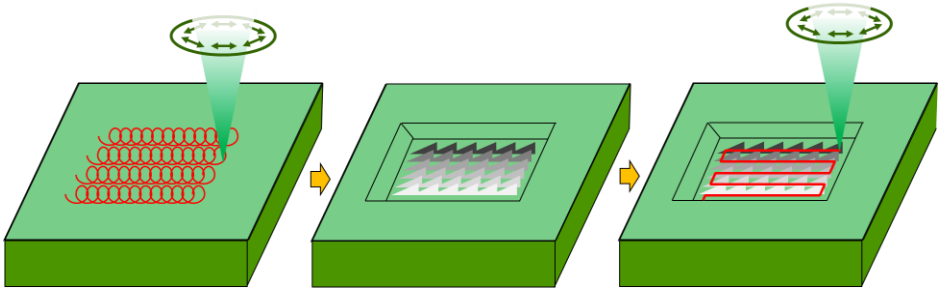

Fig. 3. Two-stage processing strategy for 4H-SiC surface machining and polishing

3. Results and discussion

3.1. Simulated surface morphology of 4H-SiC after laser slicing

Surface processing experiments were performed at energy densities of 1.25, 1.39, and 1.67 J/cm² with the following parameters: wobble tangential speed of 100 mm/s, wobble amplitude of 90 μm, overlap ratio of 99 percent, and hatch distance of 150 μm. The three-dimensional and cross-sectional morphologies obtained under these conditions are shown in Fig. 4. At 1.25 J/cm² (Fig. 4(a)), the energy density was insufficient for complete material removal, resulting in only partial processing. At 1.39 J/cm² (Fig. 4(b)), the material was uniformly removed, achieving a maximum removal depth of approximately 45 μm and an average surface roughness (Sz) of around 32.3 μm. In contrast, at 1.67 J/cm² (Fig. 4(c)), excessive energy density resulted in nonuniform removal with a maximum depth of approximately 250 μm.

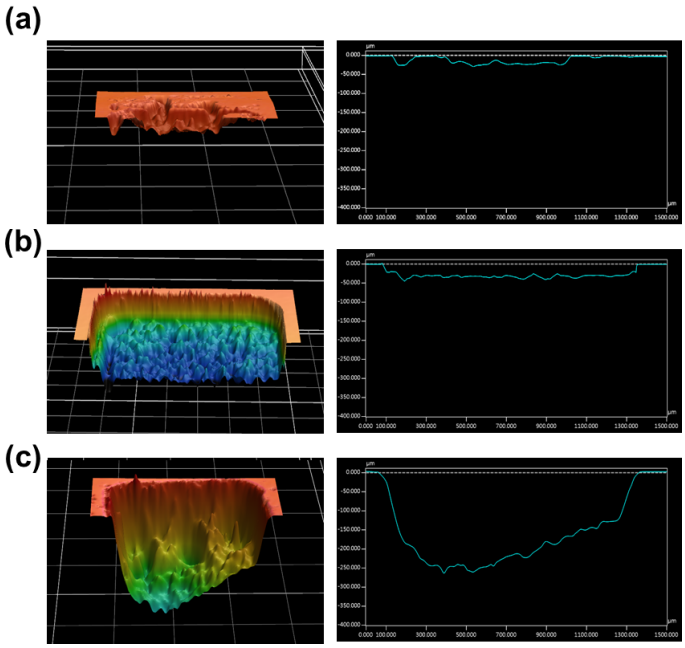

Fig. 4. Surface morphologies of 4H-SiC processed at various energy densities: (a) 1.25 J/cm², (b) 1.39 J/cm², (c) 1.67 J/cm²

SEM imaging of the sample processed at 1.39 J/cm² is shown in Fig. 5. In Fig. 5(a), uniformly distributed micron-scale protrusions are observed along the scanning trajectory. A magnified view in Fig. 5(b) reveals nano-scale particles adhering around these protrusions, with remelting occurring at their apexes (indicated by the red arrow). The annular energy distribution of the vector beam, as seen in Fig. 5(a), leads to uneven energy delivery during scanning and causes irregular material removal. The wobble scanning trajectory, however, contributes to a uniform distribution of these micron-scale features. The localized remelting is mainly caused by repeated irradiation along the wobble path, which heats the nanoparticles in the ablated regions to their melting point.

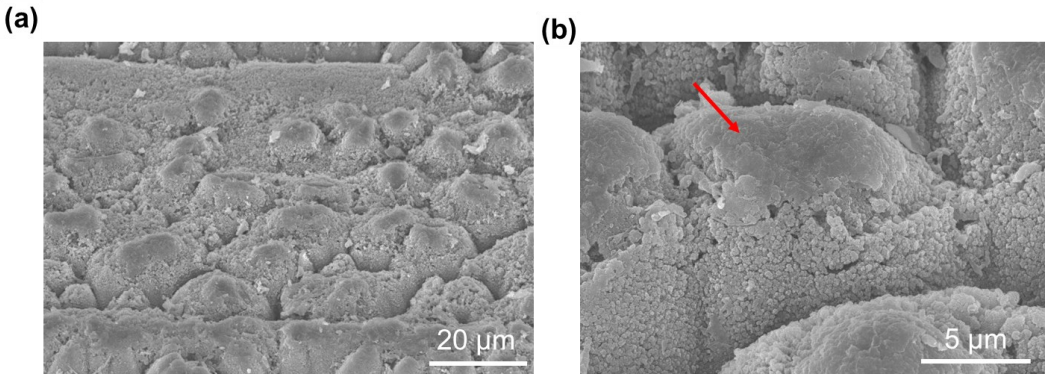

Fig. 5. (a) SEM image of 4H-SiC Processed at 1.39 J/cm²; (b) magnified image

3.2. Micro-Polishing

Laser polishing experiments were conducted on the surface produced in the first stage (see Fig. 5). Because micron-scale protrusions had formed on the 4H-SiC surface, using an energy density of 1.39 J/cm² would have increased laser absorption and enhanced material removal. Therefore, a lower energy density of 1.25 J/cm² was selected for the polishing stage in order to achieve only slight material removal on a relatively smooth surface.

Since the first stage had generated grooves of notable depth (as shown in Fig. 4(b)), the laser focal point was shifted to Z = –50 µm. Polishing was performed using a single pass setting with a hatch distance of 22 µm, as shown in Fig. 6. The results indicate that most of the micron-scale protrusions were removed, resulting in a clear reduction in overall surface roughness.

The magnified view in Fig. 6(b) further shows that in certain areas (indicated by the red arrow) nanoparticles underwent heat-induced sintering.

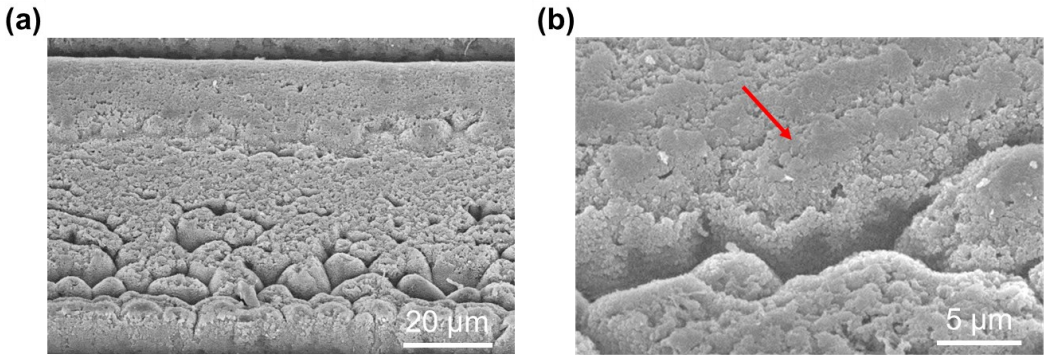

Fig. 6. (a) SEM image of 4H-SiC Processed at 1.25 J/cm²; (b) magnified image

Multiple polishing passes were performed under identical conditions. As shown in Fig. 7, the surface roughness (Sz) decreased with an increasing number of passes, reaching a minimum of approximately 9 μm after 15 passes. Each additional pass further smoothed the surface by eliminating micron-scale features and reducing deeper particle-like irregularities. However, when the number of passes was increased to 20, the roughness rose to 16 μm. This increase is attributed to the cumulative material removal, which produced pronounced processing tracks and significant height variations on the surface. SEM images after 15 passes (Fig. 8) indicate that the original micron-scale protrusions were largely eliminated, leaving only microgrooves formed by adjacent scanning tracks, while the surface exhibited a submicron-scale structural distribution (see Fig. 8(c)).

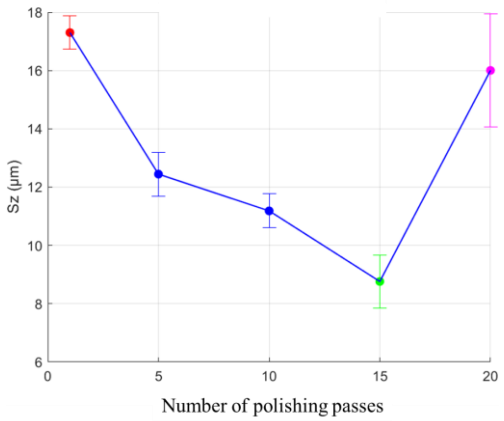

Fig. 7. Surface roughness (Sz) variation with number of polishing passes

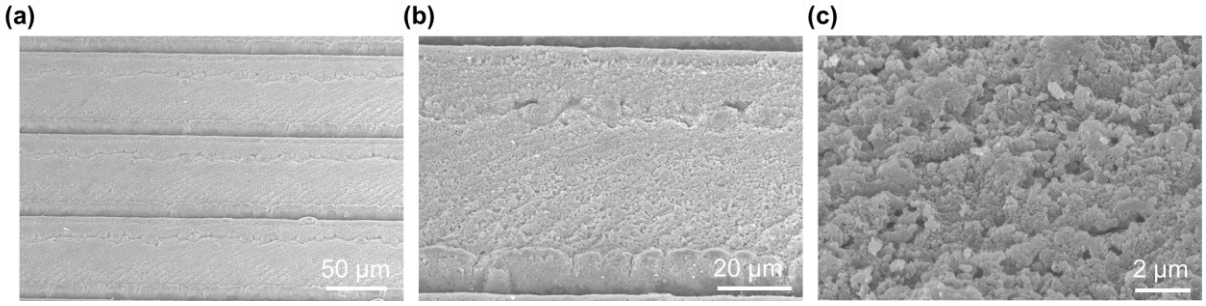

Fig. 8. (a) SEM images of 4H-SiC after 15 micro-polishing passes; (b)(c) magnified images

4. Conclusion

This study demonstrates the potential of using femtosecond laser vector beams for micro-polishing 4H-SiC surfaces. The two-stage processing approach, which first simulates the rough morphology (average surface roughness of around 32.3 µm) from laser slicing and then refines the surface via micro-polishing, proved effective in significantly reducing surface roughness. Optimal processing conditions reduced Sz to approximately 9 µm after 15 passes. However, excessive passes led to increased roughness as a result of over removal and the formation of processing tracks. These findings highlight the promise of femtosecond laser processing techniques for high-precision SiC polishing applications.

Acknowledgments

This work was supported by the National Science and Technology Council of Republic of China, under Contract NSTC 112-2221-E-A49-13 and NSTC 112-2218-E-008-010.

References

Aldeiturriaga, David Pallarés, Alain Abou Khalil, Jean-Philippe Colombier, Razvan Stoian, and Sedao Xxx. 2023. "Ultrafast vortex beams for improved energy feedthrough and low roughness surface ablation of metals." In *Laser-based Micro-and Nanoprocessing XVII*, 124090D. SPIE.

Casady, Jeffrey B, and R Wayne Johnson. 1996. 'Status of silicon carbide (SiC) as a wide-bandgap semiconductor for high-temperature applications: A review', *Solid-State Electronics*, 39: 1409-22.

Kažukauskas, Evaldas, Simas Butkus, Vytautas Jukna, and Domas Paipulas. 2024. 'Surface roughness control in deep engraving of fused silica using femtosecond laser ablation', *Surfaces and Interfaces*, 50: 104471.

Li, Yi-En, Jia-Fan Kuo, Chung-Wei Cheng, and An-Chen Lee. 2024. 'Efficient fabrication of high-quality hybrid periodic nanostructures on 4H-SiC using a single-step vector femtosecond laser processing', *Optics & Laser Technology*, 179: 111363.

Mehregany, Mehran, Christian A Zorman, Narayanan Rajan, and Chien Hung Wu. 1998. 'Silicon carbide MEMS for harsh environments', *Proceedings of the IEEE*, 86: 1594-609.

Zhang, Ru, Chuanzhen Huang, Jun Wang, Hongtao Zhu, Peng Yao, and Shaochuan Feng. 2018. 'Micromachining of 4H-SiC using femtosecond laser', *Ceramics International*, 44: 17775-83.

Zheng, Jian, Jiaxu Huang, and Shaolin Xu. 2020. 'Multiscale micro-/nanostructures on single crystalline SiC fabricated by hybridly polarized femtosecond laser', *Optics and Lasers in Engineering*, 127: 105940.